

## On microstructure-based mechanical behaviour of a ductile iron component

Ingvar L Svensson\* and Jakob Olofsson

Jönköping University, School of Engineering, Materials and Manufacturing - Casting  
P.O. Box 1026. SE-551 10 Jönköping. Sweden

Castings are produced by a manufacturing method which gives the components properties that are depending on design, metallurgy and casting method. The aim is to explore and model the local properties in a cast iron component where the properties can vary in the casting volume, which makes it difficult to optimize the castings with good accuracy.

This paper presents modelling and simulation of local microstructure-based mechanical behaviour. The mechanical behaviour can be shown as stress-strain curves at different locations of the cast iron component. A careful evaluation of tensile tests are made of three industrial components to characterize the stress – strain curves for regions holding different microstructures. This data will be used to determine the local properties and how they will influence the component behaviour at service.

**Keywords:** ductile iron, microstructure, stress-strain curves, simulation, elastic deformation, plastic deformation.

### Introduction

Castings are produced by a manufacturing method which gives the components local properties that are dependent on design, metallurgy and casting method. E.g. the wall thickness influences the resulting coarseness and type of microstructure, and the material will have local material properties which depend on the local metallurgical and thermal history. The mechanical behaviour of a cast iron component can vary significantly in the casting volume, which makes it difficult to optimize the castings with good accuracy. Structural analyses of cast products in service, e.g. using Finite Element Method (FEM) simulations, are typically based on the assumption of constant material properties throughout the product. This is not an optimal representation of the variations that are actually found in the casting. By predicting the distribution of microstructural features and establishing quantitative relationships between microstructure and mechanical behaviour, it will be possible to calculate the local material properties and the deformation behaviour of cast products with higher precision.

Previous work has presented modelling and simulation of mechanical properties related to the graphite morphology and matrix constituents using strength and strain hardening coefficients<sup>-10</sup>. A next step in this development is to get more experience of how the variation of microstructure influences the component behaviour in service life. Many questions can be raised about the stress - strain curve and its shape. To make a detailed analysis, three components with the same geometry were selected. It will be shown later that there are small differences in composition and resulting microstructure which influences the variations in mechanical behaviour. The mechanical properties can be shown as stress-strain curves at different locations of the cast iron component. The used models make it possible to determine qualitative stress-strain curves for any pearlitic cast iron grade and for pearlitic-ferritic ductile iron grades by knowing the fraction and morphology of the graphite, and the chemical composition.

The goal is to increase the understanding of how the microstructure and related mechanical properties influences the deformation behaviour of the selected component. To get the best relation between microstructure and properties, both microstructure and stress - deformation curves were analysed carefully. The characterization model and evaluated parameters were obtained by a least square method and put into a casting process simulation program.

### Experimental Procedure

The investigated component is a cast bracket for a truck engine support, illustrated in Fig. 1a. Three components were tested and analysed in respect of microstructure and mechanical properties. Seven tensile test bars were cut from each of the castings, located as illustrated in Fig. 1b.

\* Corresponding author, e-mail: ingvar.svensson@jth.hj.se



**Fig. 1:** a) CAD geometry of the engine support. 1b) Location of tensile test samples of the component. Tensile bar 1-4, 2-5 3-6 are located on each side of the component and 7 at the thin connection to the left.

The test specimens were cut out from the engine supports manually with an automated saw machine. From each support 7 specimens were taken. The final shape and dimension of the tensile specimens were obtained by sectioning the casting samples, and machined to cylindrical tensile bars with 5 mm diameter, 35 mm gauge length and 3  $\mu$ m surface finish.

The chemical composition was analysed by remelting a piece of the component to an analysis coin, which was analysed using a spectrometer. Note that some amount of Mg is lost due to the remelting. The measured chemical compositions are shown in Table 1.

**Table 1:** Chemical composition

Component	C	Si	Mn	P	S	Cr	Mo	Ni	V	Cu	Ti	Pb	Mg	Sn
C 1	3.47	3.15	0.32	0.019	0.010	0.048	0.020	0.030	0.005	0.94	0.014	0.001	0.010	0.005
C 2	3.63	3.22	0.33	0.018	0.010	0.042	0.021	0.030	0.005	0.30	0.013	0.002	0.025	0.006
C 3	3.50	3.14	0.32	0.018	0.011	0.040	0.020	0.031	0.004	0.29	0.013	0.001	0.028	0.005
Average	3.54	3.17	0.32	0.019	0.010	0.043	0.021	0.030	0.005	0.51	0.014	0.001	0.021	0.006
Stdev	0.08	0.04	0.01	0.001	0.001	0.005	0.000	0.000	0.001	0.37	0.000	0.001	0.010	0.000

Tensile tests were performed in room temperature using a Zwick/Roell Z100 uni-axial tensile testing machine with a crosshead speed of 1 mm/min. The engineering curve obtained was converted into true stress and true strain<sup>1,2</sup>. To be able to evaluate the plastic deformation, the elastic part of the true stress – strain curve was subtracted. In this paper two models to study the plastic behaviour are described. In 1945 Hollomon<sup>3</sup> introduced an empirical equation, commonly referred to as the Hollomon equation, which describes the plastic part of the true stress-strain curve until necking as

$$\sigma = K_1 \cdot (\varepsilon_{pl})^{n_1} \quad \text{Equation 1}$$

where  $\sigma$  is the true stress,  $\varepsilon_{pl}$  the true plastic strain,  $K_1$  the strength coefficient and  $n_1$  the strain hardening exponent. The strain hardening exponent describes the ability of the material to resist further deformation, and the higher the value the higher is the rate at which the material strain hardens. To determine the  $K_1$  and  $n_1$  parameters a log-log plot of the true stress-true strain data is used. Using Eq. 1 and the Considere criterion,  $d\sigma/d\varepsilon_p = \sigma$ , it can be shown that the strain hardening exponent numerically corresponds to the true plastic strain at necking,  $\varepsilon_u = n_1$ . The true total strain  $\varepsilon_{Tr}$  can be calculated as

$$\varepsilon_{Tr} = \varepsilon_{el} + \varepsilon_{pl} = \frac{\sigma}{E} + \frac{\sigma^{1/n_1}}{K^{1/n_1}} \quad \text{Equation 2}$$

For some materials, the Hollomon equation does not describe the true stress-strain curve at low strains well. By studying the deviation between the calculated and the measured true stress-strain curves a new term was added to the Hollomon expression by Ludwigson<sup>4</sup> to improve the fit, see eq. 3, where  $K_2$  and  $n_2$  are material constants [6].

$$\sigma = K_1 \cdot \varepsilon^{n_1} + \Delta \quad \text{where } \Delta = e^{(K_2 + n_2 \cdot \varepsilon)} \quad \text{Equation 3}$$

The evaluated Ludwigson equations for location 7 is shown in graphical form in Fig. 2. The remaining current results are presented in numerical form in Appendix A, and in graphical form in Appendix B.

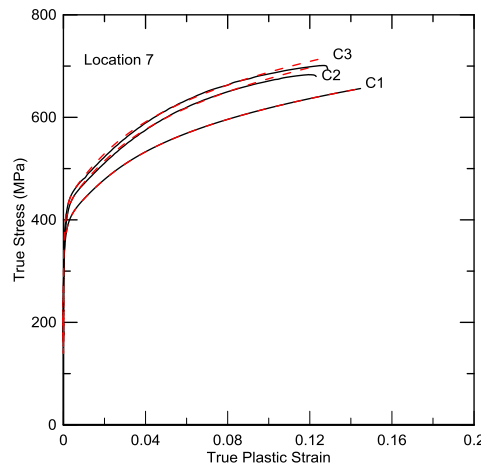


**Fig. 2:** Stress – Strain curves for location 7 with experimental curves (solid) and evaluated Ludwison curves (dashed) for component 1-3

The microstructure was evaluated in areas close to the tensile test samples. The microstructure measurements were performed by digital image analysis. The graphite morphology was first measured on a polished sample, which was then etched in Nital to determine the fractions of pearlite and ferrite. Colour etching was also applied, but is not presented in the current paper. At least 10 different measurements were made on each component and location. The results are shown in Table 2.

**Table 2:** Microstructure evaluation

Location		Fraction pearlite, P (%)	Nodularity	fgr	Round part. (%)	Nodule count, N (per mm <sup>2</sup> )
1	Average	22	72	0.159	54.2	193
	Stdv	1	3	0.003	1.5	5
2	Average	16	70	0.161	36.0	129
	Stdv	9	5	0.021	10.5	37
3	Average	25	69	0.150	22.7	81
	Stdv	2	2	0.011	4.2	15
4	Average	26	75	0.151	61.3	219
	Stdv	1	1	0.016	3.2	12
5	Average	13	65	0.148	48.1	172
	Stdv	3	4	0.025	5.8	21
6	Average	24	70	0.155	29.1	104
	Stdv	5	1	0.022	6.9	25
7	Average	27	78	0.152	84.3	301
	Stdv	4	6	0.015	2.5	9

A least square method was applied to fit a linear material characterization model relating the parameters for the Holloman and Ludwison equations with the evaluated microstructural features. The equations providing the best fit were found to be

$$n_1 = 0.1642 + 4.85 \cdot 10^{-4} \cdot P - 3.11 \cdot 10^{-5} \cdot N \quad \text{Equation 4}$$

$$K_1 = 634 + 11.89 \cdot P + 0.139 \cdot N \quad \text{Equation 5}$$

$$n_2 = -117.1 - 0.640 \cdot P - 0.084 \cdot N \quad \text{Equation 6}$$

$$K_2 = 4.50 + 1.59 \cdot 10^{-3} \cdot P + 4.44 \cdot 10^{-4} \cdot N \quad \text{Equation 7}$$

where  $P$  is fraction perlite and  $N$  nodule count as shown in Table 2.

## Results and Discussion

The modelling of the shape of the stress-strain curves provides very good fit to the experimental curves. The microstructure measurements showed small variations and normally within a standard deviation of 1-2 units of e.g. pearlite content. The optimized results for all components and locations gave a higher deviation. Some parameters are still missing in understanding of how the microstructure is related to the tensile test curve.

The next step in the procedure is the simulation of the microstructure of the component. A development version of a casting simulation program was applied to simulate the casting process and predict the microstructure formation throughout the component. The resulting microstructure is depending on the kinetics of the transformation of the austenite to ferrite and pearlite, where the overall controlling factor is the cooling rate during the transformation. The kinetics and fraction of ferrite and pearlite are depending on e.g.:

- the diffusion coefficient of carbon in ferrite and diffusion barrier at the graphite nodule surface,
- the time and temperature when the reaction can occur,
- the equilibrium temperature of ferrite and pearlite temperature
- the nucleation of ferrite and pearlite,
- the nodule count,
- the alloying contents, which affect the driving force and diffusion rate.

The ferrite and pearlite growth is, as can be seen from above rather complex in its nature. A more detailed study is shown in the work of Wessen and Svensson<sup>15</sup>.

The characterization model developed in the current work was implemented into *the closed chain of simulations for cast components*, which has been described in previous work<sup>16</sup>. In the casting process simulation the material characterization model, Eqs. 4-7, are locally applied using the simulated microstructural parameters as input. The local mechanical behaviour results were transferred into a FEM simulation of the engine support subjected to load. The geometry and load case has been previously described<sup>17</sup>. The calculated stress distribution at a certain load level is shown in Fig. 3. It has been previously shown that the local variations in mechanical behaviour are important contributions to the mechanical behaviour of the component, which a homogenous FEM simulation fails to describe<sup>17</sup>. Future studies will be aimed at comparing microstructure-based modelling using the Hollomon equation<sup>17</sup> and the current Ludwison equation, and investigate their respective relevance for different cast irons.

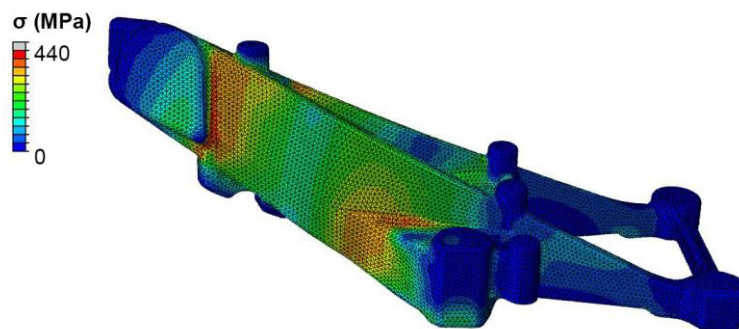


**Fig. 3:** Simulated stress distribution using microstructure-based mechanical behaviour through the derived Ludwison equation characterisation models.

## Conclusions

In the current paper a microstructure-based characterization model relating microstructural features and the parameters of the Ludwison equation have been presented. The model is found to accurately describe the different tensile behaviours found on different locations throughout the component. The model has been implemented into *the closed chain of simulations for cast components*, which is able to predict the local microstructure and mechanical behaviour and incorporate the results into FEM simulations of the component behaviour in service.

## References

1. W. Callister: 'Materials Science and Engineering', 2005, John Wiley & Sons Inc.
2. D. R. Askeland: 'The Science and Engineering of Materials', 1998, Stanley Thornes Ltd.
3. SS-EN ISO 6892-1:2009(E): *Metallic materials – Tensile testing – Part 1: Method of test at room temperature*, B. European Committee for Standardization, 2009.
4. J. H. Hollomon: *Trans. AIME*, 1945, 162, 268-290.
5. D. C. Ludwigson: *Metall. Mater. Trans. B*, 1971, 2, 2825-2828.
6. I. L. Svensson and T. Sjögren: *On modelling and simulation of mechanical properties of cast irons with different morphologies of graphite*. Carl Loper Cast Iron Symposium, Madison, Wisconsin, USA, 2009.
7. D. Larsson, T. Sjögren and I. L. Svensson: *Int. Foundry Res.*, 2008, 60, 8-16.
8. T. Sjögren and I. L. Svensson: *Int. J. Cast Met. Res.*, 2004, 17, 271-279.
9. T. Sjögren and I. L. Svensson: *Int. J. Cast Met. Res.*, 2005, 18, 249-256.
10. T. Sjögren and I. L. Svensson: *Modelling the Effect of Graphite Morphology on the Deformation of Cast Irons*. Eighth International Symposium on Science and Processing of Cast Iron (SPCI8), Beijing, China, 2006.
11. T. Sjögren and I.L. Svensson: *Metall. Mater. Trans. A*, 2007, 38, 840-847.
12. T. Sjögren, M. Wessén, I. L. Svensson and W. Schaefer: *Proc. Modeling of Casting, Welding and Advanced Solidification Processes XI*, Opio. France, 2006. pp. 685-692.
13. I. L. Svensson, S. Seifeddine, L. Elmquist, E. Sjölander and T. Sjögren: *On characterization and modelling of mechanical properties of materials for cast components*. World Foundry Congress WFC 2012, Monterrey, Mexico. 24-27 April 2012.
14. G. E. Dieter: 'Mechanical Metallurgy'. 3rd edn; 1986, New York, McGraw-Hill.
15. M. Wessén and I. L. Svensson: *Metall. Mater. Trans A*, 1996, 27A(8), 2009-2220.
16. J. Olofsson and I.L. Svensson: *Mater. Des.*, 2012, 34, 494-500.
17. J. Olofsson and I.L. Svensson: *Mater. Des.*, 2013, 43, 264-271.

## Acknowledgement

The Swedish Knowledge Foundation is greatly acknowledged for financing the research profile CompCAST in which the current paper has been refined and made. A great thanks to former master student M.Sc. Gopal Dewangan and M.Sc. Dan Larsson for preparing the samples and performing the measurements.

**Appendix A: Tensile test evaluation data****Table 1:** Result of mechanical testing

Location	Comp	UTS (MPa)	YS (MPa)	E (MPa)	eb (-)	ep (-)	n <sub>1</sub> (-)	K <sub>1</sub> (MPa)	n <sub>2</sub> (-)	K <sub>2</sub> (-)
1	C 1	555	392	169 439	0.185	0.166	0.161	884	-196	4.59
	C 2	569	400	170 896	0.119	0.109	0.176	946	-166	4.75
	C 3	559	449		0.114	0.110	0.128	826	-140	4.53
	Average	561	414	170 167	0.139	0.128	0.155	885	-167	4.62
	Stdv	7	31	1 031	0.039	0.032	0.024	60	28	0.11
2	1	496	363	165 117	0.202	0.180	0.159	780	-192	4.66
	2	517	377	168 986	0.165	0.149	0.170	840	-159	4.76
	3	536	373	163 500	0.128	0.117	0.177	894	-178	4.66
	Average	516	371	165 868	0.165	0.149	0.169	838	-176	4.69
	Stdv	20	7	2 819	0.037	0.032	0.009	57	17	0.06
3	1	565	396	169 488	0.145	0.132	0.171	924	-189	4.69
	2	550	388	167 022	0.147	0.133	0.172	901	-171	4.71
	3	527	362	156 414	0.136	0.124	0.174	873	-192	4.58
	Average	548	382	164 308	0.143	0.130	0.172	900	-184	4.66
	Stdv	19	18	6 947	0.006	0.005	0.002	26	11	0.07
4	1	575	404	170 231	0.155	0.140	0.166	932	-174	4.63
	2	578	399	163 272	0.150	0.136	0.170	942	-181	4.63
	3	556	384	156 231	0.160	0.144	0.163	895	-212	4.52
	Average	570	396	163 244	0.155	0.140	0.167	923	-189	4.59
	Stdv	12	11	7 000	0.005	0.004	0.003	25	20	0.06
5	1	488	355	159 240	0.173	0.156	0.162	778	-174	4.61
	2	501	363	165 994	0.188	0.169	0.163	797	-175	4.65
	3	488	354	156 752	0.174	0.157	0.164	783	-181	4.63
	Average	492	357	160 662	0.178	0.160	0.163	786	-177	4.63
	Stdv	7	5	4 782	0.008	0.007	0.001	10	3	0.02
6	1	529	378	161 646	0.119	0.108	0.176	892	-173	4.70
	2	519	367	159 658	0.094	0.086	0.185	908	-168	4.67
	3	561	381	167 655	0.123	0.112	0.181	950	-187	4.67
	Average	536	375	162 986	0.112	0.102	0.181	917	-176	4.68
	Stdv	22	7	4 164	0.016	0.014	0.004	30	10	0.02
7	1	558	386	163 275	0.155	0.140	0.162	898	-169	4.42
	2	608	411	172 777	0.131	0.119	0.173	1 006	-163	4.58
	3	620	426	175 089	0.140	0.127	0.166	1 008	-188	4.59
	Average	595	408	170 380	0.142	0.129	0.167	971	-173	4.53
	Stdv	33	20	6 261	0.012	0.010	0.005	63	13	0.09

eb = ultimate total strain, ep = ultimate plastic strain

**Appendix B: Tensile test curves for location 1-6.**

Results for location 7 are shown in the paper.

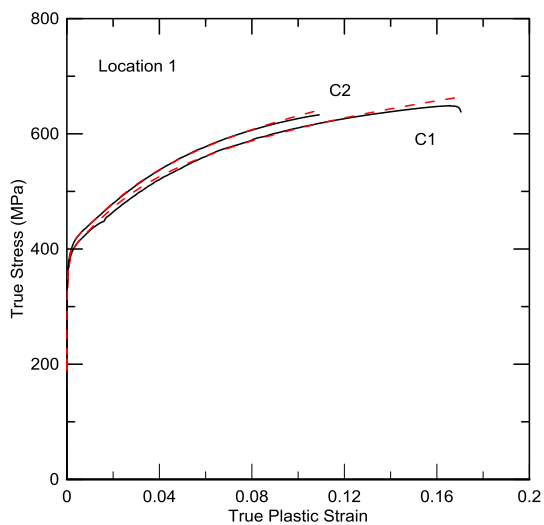


**Fig. 1:** Stress – strain curves for location 1

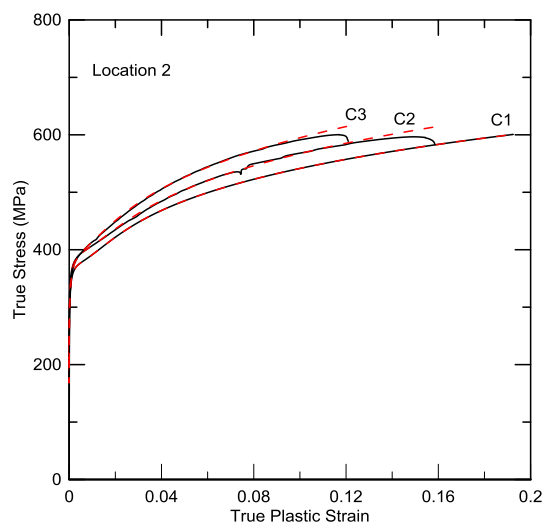


**Fig. 2:** Stress – strain curves for location 2

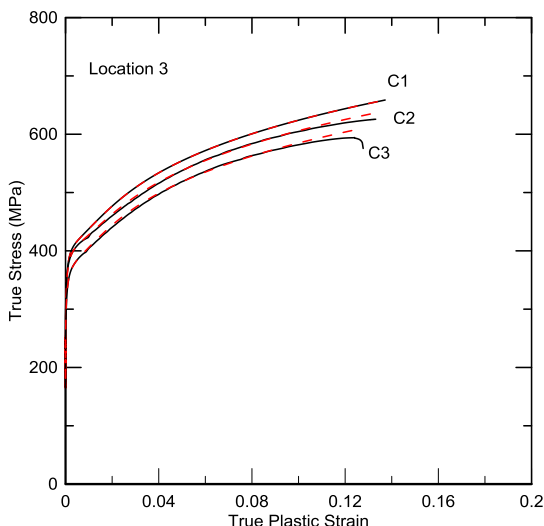


**Fig. 3:** Stress – strain curves for location 3

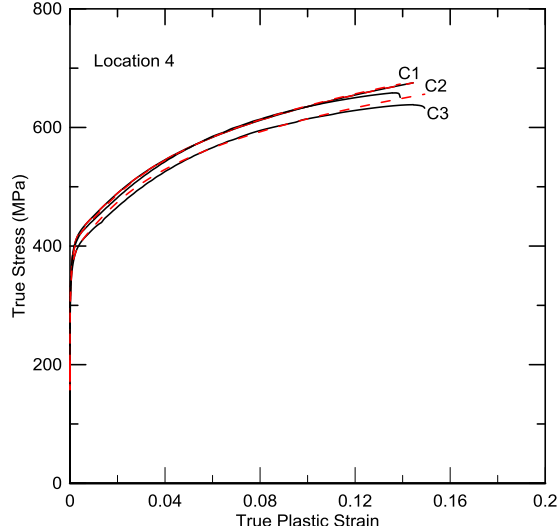


**Fig. 4:** Stress – strain curves for location 4

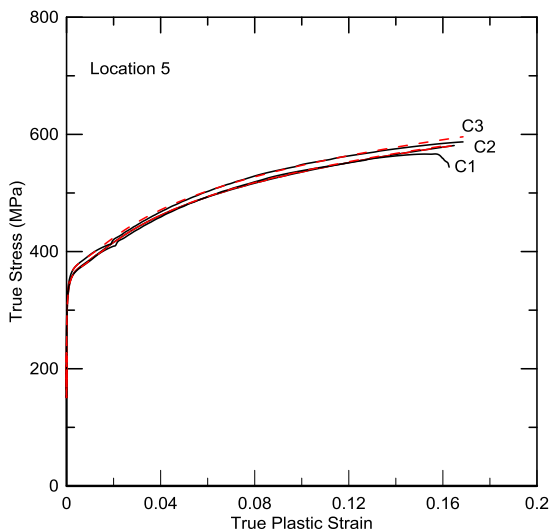


**Fig. 5:** Stress – strain curves for location 5

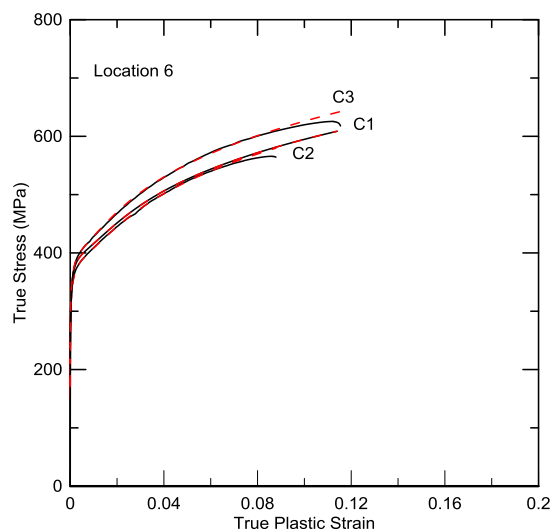


**Fig. 6:** Stress – strain curves for location 6